

Effect of metabolic syndrome on neural plasticity and morphology of the hippocampus: correlations of neurological deficits with physiological status of the rat

Zdenka Gasparova¹, Pavol Janega^{2,3}, Peter Weismann⁴, Hisham El Falougy⁴, Barbara Tyukos Kaprinay^{1,5}, Boris Liptak^{1,5}, Dominika Michalikova^{1,5} and Ruzena Sotnikova¹

¹ Institute of Experimental Pharmacology and Toxicology, Centre of Experimental Medicine, Slovak Academy of Sciences, Bratislava, Slovakia

² Institute of Pathology, Faculty of Medicine, Comenius University, Bratislava, Slovakia

³ Institute of Normal and Pathological Physiology, Centre of Experimental Medicine, Slovak Academy of Sciences, Bratislava, Slovakia

⁴ Institute of Anatomy, Faculty of Medicine, Comenius University, Bratislava, Slovakia

⁵ Institute of Pharmacology, Jessenius Faculty of Medicine, Comenius University, Martin, Slovakia

Abstract. Fat-rich diet (FRD) triggers health complications like hypertension, dyslipidemia, hyperglycemia, insulin resistance and non-alcoholic fatty liver disease, known as the risk factors of metabolic syndrome (MetS), which may result in neurological deficits. The impact of MetS on neuronal functions and brain morphology are poorly understood. We induced MetS-like conditions by exposing hypertriacylglycerolemic (HTG) rats to FRD for eight weeks with the aim to study possible neurological dysfunctions. HTG-FRD rats were compared to HTG rats and Wistar rats on standard diet. The physiological status of the animals was monitored by body, liver and kidney weight (wt). Morphology of the liver, vessel wall and hippocampus were investigated. Basal neurotransmission and synaptic plasticity were measured in the hippocampus *ex-vivo*. A marked increase of liver weight with marks of steatosis was found in the HTG-FRD group. FRD induced an increase of aortic *intima-media* thickness. Extracellular recording revealed FRD-induced impairment of long-term potentiation (LTP) at *Cornu Ammonis* (CA)3-CA1 synapse, contrary to increased presynaptic fiber volley (pV). Reduced thickness of pyramidal cell layer at the CA1 area was found morphometrically. LTP was directly associated with kidney weight and inversely associated with liver weight, pV directly correlated with liver weight, liver wt/body wt ratio and aortic *intima-media* thickness. Our results suggest correlations between altered physiological status due to MetS-like conditions and neurological deficits, which may be related with consecutive development of so-called metabolic cognitive syndrome.

Key words: Hippocampus — Neurotransmission — Liver — Abdominal aorta — Fat-rich diet

Abbreviations: ACSF, artificial cerebrospinal fluid; AD, Alzheimer disease; CA, *Cornu Ammonis*; CV, central vein; ECD, equivalent circle diameter; EPSP, excitatory postsynaptic potential; FRD, fat-rich diet; H-E, hematoxylin-eosin; HTG, hypertriacylglycerolemic rats; LTP, long-term potentiation; MetS, metabolic syndrome; OD, optical density; PoS, population spike; PS, portal space; pV, presynaptic fiber volley; SD, standard diet; TAG, triacylglycerol; TC, total cholesterol; wt, weight.

Introduction

In the last decades, a sedentary form of life accompanied by increased intake of food with high fat and sugar content has resulted in increased prevalence of metabolic syndrome (MetS). The concept of MetS was introduced in 1988 (Reaven 1988) and since then various definitions were proposed by the World Health Organization, the European Group for Study of Insulin Resistance, the National Cholesterol Education Program Adult Treatment Panel III., etc. Generally accepted, MetS is clinically manifested by the presence of a cluster of simultaneous risk factors (at least three of them), including hypertension, dyslipidemia, hyperglycemia, insulin resistance, increased waist circumference, endothelial dysfunction, increased inflammatory reactions and markers of oxidative stress (Grundy 2007; Huang 2009). Risk factors of MetS have been suggested not to be independent of one another; they have common causes, mechanisms and features (Grundy et al. 2005; Huang 2005, 2009; Kahn et al. 2005; Grundy 2007).

Coincidence of MetS risk factors and impairment of cognitive functions with degenerative or vascular origin starts to be identified as the metabolic cognitive syndrome (Panza et al. 2012). However, the research field of association of metabolic risk factors and cognitive impairment or brain pathological changes is still little explored (Schwarz et al. 2017). It was documented that obesity and insulin resistance are risk factors for the development of Alzheimer disease (AD) (Craft 2005). Increased levels of cholesterol in plasma correlate with increased risk for AD (Vance 2012). Vascular factors, especially hypertension, a high level of cholesterol in mid-life, and diabetes are risk factors for AD and are thought to promote the production of beta-amyloid (Sjögren and Blennow 2005). MetS represents a risk factor for cognitive decline and vascular dementia in older age (Siervo et al. 2014). People with MetS have an increased risk of stroke (Hansen et al. 2008). Some components of MetS have a negative influence on cognitive abilities (Fanjiang and Kleinman 2007; Hassenstab et al. 2009; Kanoski and Davidson 2010) and an increased risk of dementia (Muller et al. 2007). Coincidence of certain risk factors may have a synergistic effect and result in specific cognitive and brain abnormalities connected with MetS (Hwang et al. 2010; Boitard et al. 2012; Valladolid-Acebes et al. 2012). Consumption of diet, high in saturated fat and added sugars, impairs the blood brain barrier and negatively impacts cognitive functions, particularly mnemonic processes that rely on the integrity of the hippocampus (Noble et al. 2017).

As the health complications accompanying MetS are serious, many studies have been done on animal models to mimic features of the development and maintenance of MetS. The research is aimed at the study of pathological mechanisms, treatment and finally at health improvement of humans with MetS. Experimental models of MetS may

be genetic, chemically-induced, or diet-induced (Lehnen et al. 2013). To mimic MetS-like conditions, the model of hypertriacylglycerolemic (HTG) rats was established (Zicha et al. 2006). Moreover, we found and published recently (Kaprinay et al. 2016) that hypertriacylglycerolemia of these rats combined with fat-rich diet (FRD) resulted in markedly disturbed lipid metabolism expressed by increased total cholesterol and low-density lipoprotein-cholesterol, decreased high-density lipoprotein-cholesterol and disturbed glucose metabolism, compared to HTG rats fed standard diet (SD). These changes in the serum lipidic profile were accompanied with oxidative stress and tissue damage identified as increased liver concentrations of thiobarbituric acid reactive substances and increased specific activity of the lysosomal enzyme N-acetyl- β -D-glucosaminidase.

Based on dyslipidemia and increased oxidative stress as a result of hypertriacylglycerolemia of HTG rats combined with FRD (Kaprinay et al. 2016), we hypothesized that neurological deficits could manifest under these stronger experimental conditions for induction of MetS. The aim of this work was thus to compare this improved model for MetS (HTG rats fed FRD) with the initial approach suggested for MetS study model (HTG rats fed SD) (Zicha et al. 2006). Further, we compared both groups of HTG rats with healthy control Wistar rats, as the HTG rats actually originate from them. Based on our preliminary knowledge about low sensitivity of Wistar rats to 1% cholesterol and 7.5% lard diet (not published), we did not deal with Wistar rats fed FRD. As generally accepted markers for confirmation of the presence of MetS are e.g. manifestations of nonalcoholic fatty liver disease, impaired vascular elasticity, atherosclerosis, hypertension, kidney deficits, etc. (Paschos and Paletas 2009), we focused on the characterization of the physiological status of the animals tested. The aims of this paper were as follows: 1) to monitor body, liver and kidney weights, extent of liver steatosis and vascular wall thickness, 2) to investigate the presence of putative neurological function deficits in the hippocampus, a brain structure associated with memory and cognition, 3) to support neurological dysfunctions with putative morphometrical changes in the hippocampus, 4) and finally to demonstrate possible correlations of neurological deficits in the hippocampus with changes in the physiological status elicited by MetS-like conditions.

Material and Methods

Animals and diet

All experimental procedures involving animals were approved by the Ethical Committee of the Institute of Experimental Pharmacology and Toxicology, Animal Health and Animal Welfare Division of the State Veterinary and Food

Administration of the Slovak Republic (the number of the permit 3635/14-221) and they conformed to Directive 2010/63/EU on protection of animals used for scientific purposes. Adult male Wistar and HTG rats aged 12 weeks ($n = 30$, weight 243 ± 6 g at the onset of the experiment) from the Breeding Station of the Institute of Experimental Pharmacology and Toxicology (Dobra Voda, Slovakia) were used. The rats had free access to water and food and were kept on 12h/12h light/dark cycle and housed 5 animals *per* cage. Wistar rats were fed SD (Wistar-SD, $n = 10$); and HTG rats were fed SD (HTG-SD, $n = 10$) or FRD (HTG-FRD, $n = 10$).

Standard rodent diet was produced by the certified producer of pellets at the Department of Toxicology and Breeding of Laboratory Animals, Institute of Experimental Pharmacology and Toxicology, Centre of Experimental Medicine, Slovak Academy of Sciences, Dobra Voda, Slovakia, which is registered under the number α SK 100089, code 6147. Composition of the SD: wheat, processed animal protein, oat, barley-corn, extruded lucerne, soybean extracted grit, wheat bran, wheat germs, mineral mix, vegetable oil, natrium chloride. Added vitamins *per* 1 kg: E 672 vitamin A – 20,000 IU; E 671 vitamin D3 – 2,000 IU; vitamin E – 70 mg; added amino acids *per* 1 kg: DL-methionine – 1.2 g; L-lysine – 0.8 g. Analytical components: 19.10% nitrogen substances; 3.60% fiber; 5.10% oil and fat; 5.85% ash; 9.10% humidity. FRD was enriched by 1% cholesterol and 7.5% lard and was given for eight weeks. The amount of consumed food was recorded each day as the difference between added and rest weight of food *per* cage, and recalculated to the consumed food in g/rat/day (mean \pm SEM). The energetic value of the consumed food was expressed as kJ/rat/day (mean \pm SEM). The rat body weight was monitored once a week.

After eight weeks of experiment, one rat from each of the three experimental groups was terminated *per* day by decapitation under ether anesthesia. Terminations of rats from three experimental groups were randomized and carried out from 9:00 to 10:00 a.m. The brain was quickly removed from the skull and the left hippocampus was used for electrophysiology. The liver and both kidneys were weighed. The right hippocampus and samples of liver and abdominal aorta were collected for further morphometric determinations.

Liver

Formalin fixed and paraffin embedded specimens of the liver were standardly sectioned ($5 \mu\text{m}$) and stained with hematoxylin and eosin (H-E) and microscopically examined to determine the presence of morphological alterations. Computer-labeled empty places on histological liver sections were sorted by image analysis according to sphericity and shape factor parameters. Following short visual inspection, the unwanted objects (vessels, micro-ruptures) were

removed from the image rating. Subsequently, an extent of the area of the remaining objects (microvesicles) was measured (Liquori et al. 2009). Optical density was determined on the principle that steatotic hepatocyte is lighter in H-E staining than healthy hepatocyte. The cytoplasmic density was determined by digital morphometry (ImageJ software 1.46b, National Institutes of Health, USA).

Aorta

Formalin fixed and paraffin embedded specimens of the abdominal aorta of about 10 mm length, stained with H-E, were sectioned ($5 \mu\text{m}$) perpendicularly to the axis of the vessel and microscopically examined to determine the *intima media* thickness by standardized morphometry (Tonar et al. 2015). Using the computer mouse, the adventitia was deleted in the image. By segmentation technique, thresholding, the area of the *tunica intima* together with the *tunica media* was labeled by red color and the area of the vascular lumen by green color. The morphometric software (Olympus Cell F) calculated the data of the equivalent circle diameter (ECD), i.e. the diameter of the circle that has an area equal to the area of a particle/object, particularly for the area of the intima and media, and particularly for the area of the lumen. By subtracting the small inner circle diameter (ECD₂) from the large outer one (ECD₁) and dividing it by 2, the average thickness of the *intima media* wall of the evaluated vessel was obtained (Tonar et al. 2015).

Hippocampus

Formalin fixed and paraffin embedded specimens of the right brain hemisphere sectioned by the oblique sagittal section of the brain in the midline were standardly sectioned ($4 \mu\text{m}$) and stained with H-E to prepare slices. The *Cornu Ammonis* (CA)1 area of the hippocampus was selected and captured by optical microscope (Leica DM 2000, Wetzlar, Germany) with attached camera (S50, Canon, Japan), using the final magnification 400 \times in three captured microscopic fields. The width of the pyramidal cell layer in the CA1 area from the top to the bottom line of the pyramidal cell layer of the CA area, expressed in micrometers, was determined at three sites in each captured microscopic field by digital morphometry using ImageJ software (1.46b, National Institutes of Health, USA). The number of cells in the CA1 area was counted in each captured field and expressed as the number *per* 100 μm (Abramoff et al. 2004).

Preparation of hippocampal slices and electrophysiological measurement

Hippocampal slices were prepared using a technique described in our previous (Gasparova et al. 2014). Briefly, hippocampal

slices (400 μm) cut by tissue chopper (McIlwain Tissue Chopper, Stoelting, USA) were displaced individually by wet brush into ice cold artificial cerebrospinal fluid (ACSF) solution. Then the slices were positioned by plastic suction pipette on fin filter papers (3 \times 4 mm) lying on a supporting nylon mesh separating liquid and gas phases in the incubation chamber at $33 \pm 1^\circ\text{C}$. The aqueous phase consisted of ACSF composed in mmol/l of: NaCl 124, KCl 3.3, KH_2PO_4 1.25, MgSO_4 2.4, CaCl_2 2.5, NaHCO_3 26, glucose 10 and saturated with 95% O_2 + 5% CO_2 , at pH 7.4, and the gas phase consisted of 95% O_2 + 5% CO_2 . Both phases were continuously flowing through the incubation and experimental chambers. For each electrophysiological measurement, one hippocampal slice lying on fin filter paper was displaced from incubation to the experimental chamber with the same experimental conditions and temperature. Electrophysiological measurements were performed on randomly selected slices from three experimental groups at the time from 11:00 to 19:00 p.m. Bipolar wire electrodes were used to stimulate extracellularly Schäffer collaterals evoking activity in the CA1 area trans-synaptically. Somatic response in the rat hippocampus was recorded in the *stratum pyramidale* and dendritic response was recorded in the *stratum radiatum* of the CA1 region by a glass microelectrode with the tip resistance 3–5 M Ω , pulled by microelectrode puller (Development Workshops, Slovak Academy of Sciences, Slovak Republic) and filled with ACSF. Based on our previous experiences, the stimulus intensity used was in the range from 10 to 30 V to induce somatic response and from 6 to 10 V to induce dendritic response with stimulus duration of 0.1 ms and stimulus frequency of 0.2 Hz. Recordings were amplified, visualized on the oscilloscope (Tektronix 2230, Tectronics Inc., USA) along with digitalization by the DigiData 1322A (Molecular Devices, USA) with sampling rate of 10 kHz recorded by the software AxoScope 10.3. Synaptic waveforms were stored on personal computer and further analyzed by Clampfit 10.3 software (Molecular Devices, USA). Population spike (PoS) or excitatory postsynaptic potential (EPSP) were recorded from CA1 neurons in rat hippocampal brain slices in response to Schäffer-collateral fiber stimulation. Recording of response was repeated five times in the given stimulus intensity and the average response was calculated. Somatic response was evaluated by measuring the amplitude of PoS as a parameter for sizing neuronal vitality, recorded in the *stratum pyramidale*. PoS amplitude was determined as a Δ value between two cursors placed to the most negative and the most positive points of the composed action potential trace. Dendritic response was evaluated by measuring the slope of field EPSP recorded in the *stratum radiatum*. The EPSP slope was determined by two cursors placed on the initial linear negative segment of the trace. The presynaptic fiber volley (pV) potential, as an index of the density of afferent fibers/axons that are activated to give rise to a synaptic response, was also investigated. The pV potential was characterized by its slope, measured by two cursors placed

to the middle linear part of the pV trace. Stimulus-response curves were constructed as 1) PoS amplitude expressed in mV (means \pm SEM) versus increasing stimulation intensity from 10–30 V; 2) EPSP slope expressed in mV/ms (means \pm SEM) versus increasing stimulation intensity from 6–10 V, and 3) pV slope expressed in mV/ms (means \pm SEM) versus increasing stimulation intensity from 6–10 V. Stimulus-response curves were compared within three experimental groups at given stimulus intensity points.

Further, synaptic plasticity measured by long-term potentiation (LTP) of electrically evoked response was recorded in the *stratum radiatum* of the CA1 area. The baseline response was set to 30–50% of the maximal EPSP amplitude with stimulus frequency of 0.033 Hz. After 10–15 min of a stabilization period, LTP was induced by a single train of high frequency stimulation (HFS; 100 Hz, 1 s). Immediately after LTP induction, evoked responses were recorded with baseline stimulus frequency for the following 45 min. Average baseline response expressed by EPSP slope, recorded during 10 min before HFS, was normalized to 1 and consequently all further responses were recalculated to normalized values. Individual hippocampal slices were measured from each animal of three experimental groups randomly and all recordings were performed consecutively from 11:00 h to 19:00 h as follows: at least two slices *per rat* to record PoS, at least two slices *per rat* to record EPSP, and one slice *per rat* to record LTP. Altogether about 15 hippocampal slices were measured daily, where one rat of each of the three groups was tested.

Data analysis

The data were statistically evaluated using the InStat software ver. 2.05 and GraphPad Prism software. Data were expressed as means \pm SEM. One-way analysis of variance (ANOVA) was used to evaluate the difference among all experimental groups (Tukey-Kramer multiple comparison test), the difference compared to controls (Dunnett multiple comparison test) and further the Kruskal-Wallis test were used. The level of $p < 0.05$ was considered a statistically significant difference. Linear correlation was performed on individual samples to evaluate the association between two variables (x, y). Correlations were determined by the correlation coefficient (r), where $|r(x, y)| \leq 0.3$ was considered a low correlation, $0.3 < |r(x, y)| \leq 0.8$ was considered a middle correlation and $|r(x, y)| > 0.8$ a high correlation.

Results

Effect of FRD consumption on physiological status expressed by body, liver and kidney weight of rats and liver steatosis

At the onset of the experiment, the average rat body weight ($n = 10$ rats/group) did not differ significantly between

the three experimental groups tested (Table 1; One-way ANOVA, Tukey-Kramer multiple comparisons test). The amount of food consumed on average daily during eight weeks of experiment, expressed in g/rat/day, did not differ significantly in the three experimental groups tested (Table 1; One-Way ANOVA, Tukey-Kramer multiple comparisons test). The average daily energy intake of food expressed in kJ/rat/day was significantly higher in HTG-FRD rats relative to both groups fed SD (Table 1; $p < 0.001$; One-way ANOVA, Tukey-Kramer multiple comparisons test). Regardless of higher energy intake, only a slight non-significant increase of body weight gain was observed after eight weeks of diet in the HTG-FRD group (Table 1; One-way ANOVA, Tukey-Kramer multiple comparisons test).

In spite of no effect of FRD on body weight gain, an enormous increase of liver weight (60%) was observed in HTG-FRD rats compared to both groups fed SD (Table 1; $p < 0.001$, One way ANOVA, Tukey-Kramer multiple comparisons test). Similarly, an increased liver wt/body wt ratio (%) was found in both groups of HTG rats compared to Wistar-SD rats (Table 1; $p < 0.001$, One way ANOVA, Tukey-Kramer multiple comparisons test). FRD resulted in markedly increased liver wt/body wt ratio (%) in HTG-FRD rats compared to HTG-SD (Table 1; $p < 0.001$, One way ANOVA, Tukey-Kramer multiple comparisons test). Histological H-E stained liver preparations were investigated (Fig. 1A). Presence of steatosis was determined quantitatively and expressed as percentage of steatosis area (Fig. 1B). An increased steatosis

area was found in both groups of HTG rats compared to Wistar-SD group ($* p < 0.05$ Wistar-SD vs. HTG-SD; $*** p < 0.001$ Wistar-SD vs. HTG-FRD, Kruskal-Wallis test). The FRD resulted in enormous increase in the liver steatosis area (up to 25%) in HTG-FRD group compared to HTG-SD rats ($### p < 0.001$, Kruskal-Wallis test). Determination of optical density revealed decreased ratio of light vs. dark area in HTG-SD and HTG-FRD rats compared to Wistar rats ($*** p < 0.001$, Kruskal-Wallis test). FRD resulted in further significant decrease of optical density in HTG-FRD rats ($# p < 0.05$, Kruskal-Wallis test).

Both groups of HTG rats had low kidney weight compared to Wistar-SD rats without reference to diet (Table 1; $p < 0.001$ Wistar-SD vs. HTG-SD; $p < 0.01$ Wistar-SD vs. HTG-FRD; One way ANOVA, Tukey-Kramer multiple comparisons test). Significantly decreased kidney wt/body wt ratio (%) was observed in both groups of HTG rats compared to Wistar-SD rats (Table 1; $p < 0.05$, One way ANOVA, Tukey-Kramer multiple comparisons test).

FRD induced changes in the intima-media thickness of rat abdominal aorta

The abdominal aortic sections stained with H-E were reviewed and representative aortic rings from each experimental group are shown in Fig. 2A. The vessel wall thickness from the endothelial surface to the adventitia was monitored by morphometric software in the three experimental groups

Table 1. Effect of fat-rich diet on the listed parameters

	Wistar-SD (<i>n</i> = 10)	HTG-SD (<i>n</i> = 10)	HTG-FRD (<i>n</i> = 10)
<i>Rat body weight</i>			
Onset of experiment (g)	254.9 ± 10.4	237.7 ± 11.6	236.4 ± 11.8
End of experiment (g)	396.3 ± 8.3	362.4 ± 11.8	377.2 ± 8.9
Weight gain (%)	57.2 ± 5.5	53.8 ± 3.7	61.8 ± 5.4
<i>Food consumption</i>			
Amount (g/rat/day)	25.3 ± 0.6	25.5 ± 0.6	26.9 ± 0.7
Energy intake (kJ/rat/day)	363.5 ± 8.0	365.7 ± 9.1	435.0 ± 11.6 ^{***,###}
<i>Liver</i>			
Liver weight (g)	11.27 ± 0.26	11.93 ± 0.32	18.23 ± 0.50 ^{***,###}
Liver wt/body wt (%)	2.85 ± 0.05	3.30 ± 0.06 ^{***}	4.83 ± 0.07 ^{***,###}
<i>Kidney</i>			
Both kidneys weight (g)	2.18 ± 0.06	1.86 ± 0.05 ^{***}	1.94 ± 0.05 ^{**}
Kidney wt/body wt (%)	0.55 ± 0.01	0.52 ± 0.01 [*]	0.51 ± 0.01 [*]

The experiment with diet lasted eight weeks. Animals were 5-month-old at the end of the experiment. Values are means ± SEM. $* p < 0.05$ and $*** p < 0.001$ Wistar-SD vs. HTG-SD (One-way ANOVA, Tukey-Kramer multiple comparison test); $* p < 0.05$, $** p < 0.01$ and $*** p < 0.001$ Wistar-SD vs. HTG-FRD (One-Way ANOVA, Tukey-Kramer multiple comparison test); $### p < 0.001$ HTG-SD vs. HTG-FRD (One-Way ANOVA, Tukey-Kramer multiple comparison test). Wistar-SD, Wistar rats fed standard diet; HTG-SD, hypertriacylglycerolemic rats fed standard diet; HTG-FRD, hypertriacylglycerolemic rats fed fat-rich diet; *n*, number of rats; wt, weight.

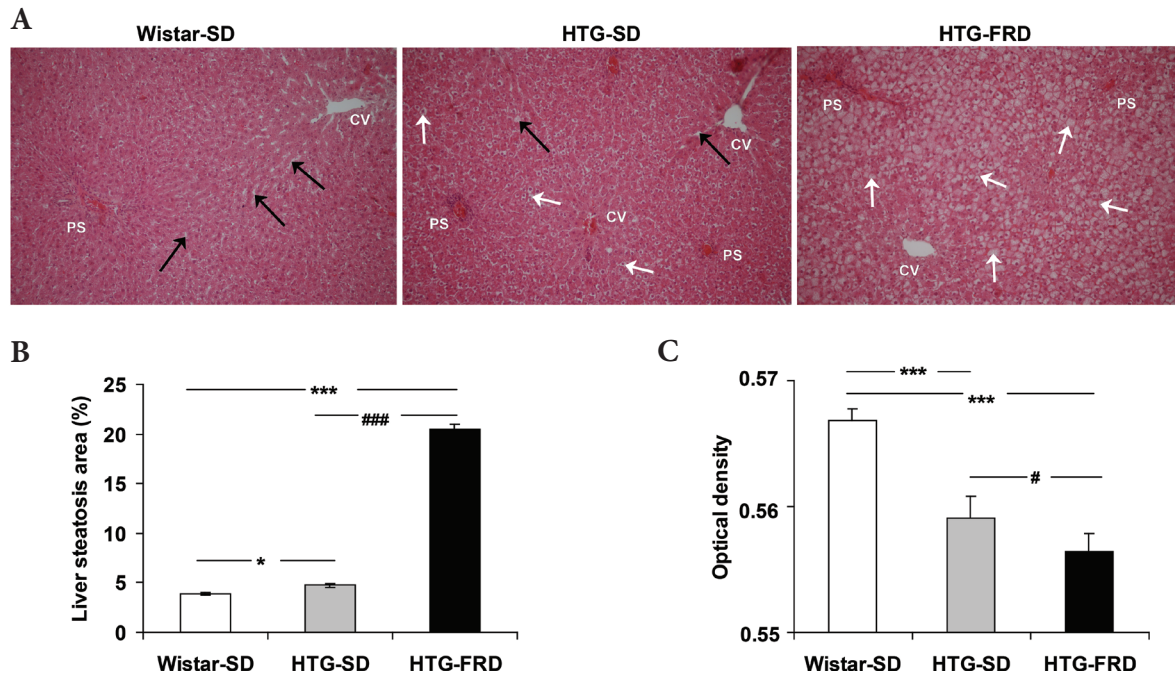


Figure 1. Effect of fat-rich diet (FRD) on the rat liver steatosis. **A.** Representative figures of hematoxylin-eosin stained liver sections of each experimental group. Black arrows indicate liver sinuses; white arrows indicate steatosis. Magnification 20 \times . **B.** Graph shows extent of steatosis area (%) in three experimental groups: Wistar-SD ($n = 97$), HTG-SD ($n = 59$), HTG-FRD ($n = 76$). * $p < 0.05$ Wistar-SD vs. HTG-SD; *** $p < 0.001$ Wistar-SD vs. HTG-FRD; ### $p < 0.001$ HTG-SD vs. HTG-FRD; Kruskal-Wallis test. **C.** Optical density in three experimental groups: Wistar-SD ($n = 97$), HTG-SD ($n = 59$), HTG-FRD ($n = 76$). *** $p < 0.001$ Wistar-SD vs. HTG-SD and Wistar-SD vs. HTG-FRD; # $p < 0.05$, HTG-SD vs. HTG-FRD; Kruskal-Wallis test. Wistar-SD, Wistar rats fed standard diet; HTG-SD, hypertriacylglycerolemic rats fed standard diet; HTG-FRD, hypertriacylglycerolemic rats fed fat-rich diet; PS, portal space; CV, central vein; n , number of liver sections.

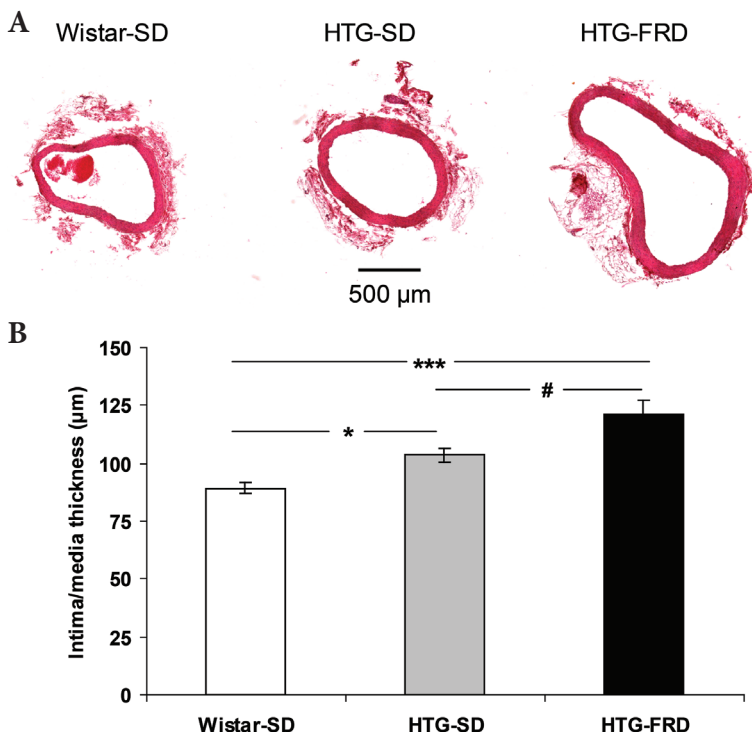


Figure 2. Effect of FRD on *intima-media* thickness of rat abdominal aorta. **A.** Illustrative hematoxylin-eosin stained aortic rings of each experimental group. **B.** Graph shows *intima-media* thickness in three experimental groups. Values are means \pm SEM of $n = 10$ rats/group. Significant difference Wistar-SD vs. HTG-SD rats * $p < 0.05$; Wistar-SD vs. HTG-FRD *** $p < 0.001$; HTG-SD vs. HTG-FRD # $p < 0.05$; One-Way ANOVA, Tukey-Kramer multiple comparisons test. For abbreviations, see Fig. 1.

tested ($n = 10$ rats/group). HTG-SD rats showed significantly increased *intima-media* thickness compared to Wistar-SD rats ($p < 0.05$, One way ANOVA, Tukey-Kramer multiple comparisons test) and consumption of FRD resulted in further increase in the aortic *intima-media* thickness of HTG-FRD rats compared to both groups fed SD (Fig. 2B; $p < 0.001$ vs. Wistar-SD, $p < 0.05$ vs. HTG-SD, One way ANOVA, Tukey-Kramer multiple comparison test).

Effect of FRD on basal neurotransmission and synaptic plasticity in rat hippocampus

Electrically evoked responses at the *Cornu Ammonis* 3 (CA3)-CA1 synapse were measured extracellularly in rat hippocampal slices. Typical somatic PoS traces recorded in the *stratum pyramidale* are shown in Fig. 3A. Stimulus-response curves were made (Fig. 3B). The somatic PoS amplitudes were slightly lower in both HTG groups of rats

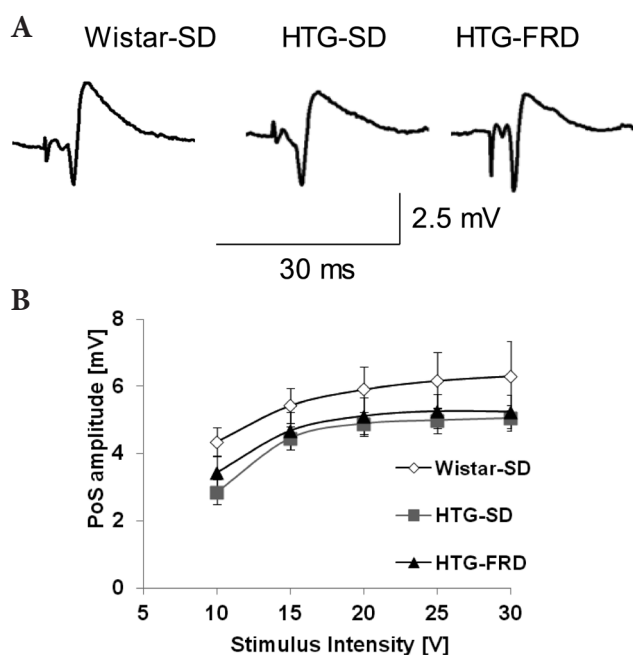


Figure 3. Effect of FRD on population spike (PoS) amplitude in the rat hippocampus. **A.** Typical individual traces of electrically evoked somatic PoS recorded as a response to maximal stimulus intensity tested (30 V; stimulus duration of 0.1 ms) in the *stratum pyramidale* of the hippocampus of the rat from each experimental group acquisitioned by AxoScope 10.3 software (Molecular Devices, USA). **B.** Stimulus-response curves of the PoS amplitude vs. stimulus intensity recorded in three experimental groups. Values are means \pm SEM of $n = 25$ hippocampal slices in Wistar-SD, $n = 25$ in HTG-SD, and $n = 21$ in HTG-FRD. Non-significant difference by One-Way ANOVA, Tukey-Kramer multiple comparisons test and Dunnett multiple comparisons test with Wistar-SD as control. For abbreviations, see Fig. 1.

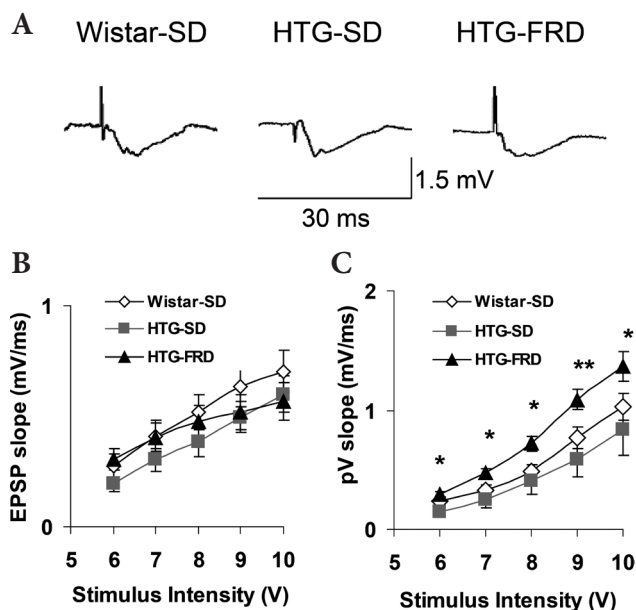


Figure 4. Effect of FRD on excitatory postsynaptic potential (EPSP) in the rat hippocampus. **A.** Typical individual traces of the field EPSP recorded as a response to maximal stimulus intensity tested (10 V, 0.1 ms) in the *stratum radiatum* of the rat hippocampus of each experimental group acquisitioned by AxoScope 10.3 software (Molecular Devices, USA). **B.** Stimulus-response curves of the EPSP slope vs. stimulus intensity recorded in three experimental groups. **C.** Stimulus-response curves of the slope of presynaptic fiber volley (pV) potential vs. stimulus intensity recorded in three experimental groups. Values are means \pm SEM of $n = 22$ hippocampal slices in Wistar-SD, $n = 23$ in HTG-SD and $n = 19$ in HTG-FRD. Significant difference between HTG-FRD vs. HTG-SD, * $p < 0.05$ and ** $p < 0.01$, One-way ANOVA, Tukey-Kramer multiple comparisons test. For abbreviations, see Fig. 1.

but they did not differ significantly compared to Wistar rats ($n = 10$ rats/group; Wistar-SD $n = 25$ hippocampal slices, HTG-SD $n = 25$ hippocampal slices, HTG-FRD $n = 21$ hippocampal slices; One way ANOVA, Tukey-Kramer multiple comparisons test, Dunnett multiple comparisons test). Typical dendritic EPSP traces recorded in the *stratum radiatum* are shown in Fig. 4A.

The EPSP slope recorded in the *stratum radiatum* was slightly reduced in HTG-FRD but there were no significant differences among the three groups tested (One-way ANOVA, Tukey-Kramer multiple comparisons test; $n = 10$ rats/group; Wistar-SD $n = 23$ hippocampal slices, HTG-SD $n = 22$ hippocampal slices, HTG-FRD $n = 21$ hippocampal slices) (Fig. 4B). We however noticed a markedly increased slope of pV potential in the dendritic CA3-CA1 hippocampal responses in HTG-FRD rats (Fig. 4C) (at all stimulus intensities $p < 0.05$ HTG-SD vs. HTG-FRD; at stimulus intensity of 9 V $p < 0.01$ HTG-SD vs. HTG-FRD;

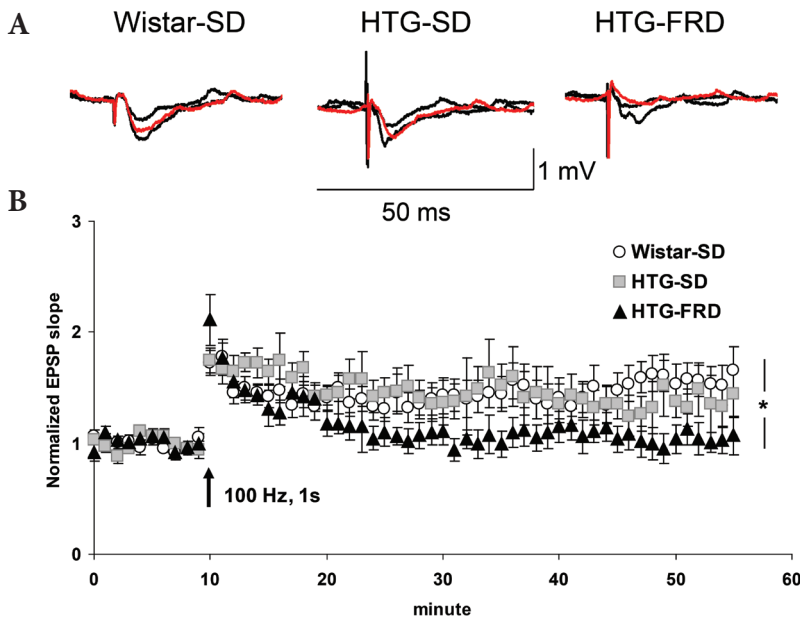


Figure 5. Effect of FRD on long-term potentiation (LTP) in the rat hippocampus. **A.** Typical individual traces of field excitatory postsynaptic potentials (EPSP) recorded in the *stratum radiatum* of the hippocampus of the rat from each experimental group acquisition by AxoScope 10.3 software. Superimposed traces are as follows: EPSP with the smallest amplitude represents response recorded during stabilization period, EPSP with the highest amplitude represents induction of LTP, thus response recorded immediately after high frequency stimulation (HFS; 100 Hz, 1 s), and the red trace represents EPSP recorded 45 min after HFS in the hippocampus of Wistar-SD, HTG-SD or HTG-FRD. **B.** The normalized EPSP slope values of electrically evoked responses at the CA3-CA1 synapse, recorded in the *stratum radiatum* during a 10-min stabilization period (stimulation at 0.033 Hz; stimulus duration of 0.1 ms), during LTP induction by a single train of HFS (100 Hz, duration of 1 s) and for further 45 min at the

baseline stimulation mode. The slope of EPSP dropped to baseline values within about 15–20 min after HFS in HTG-FRD rats. Values are means \pm SEM of $n = 10$ hippocampal slices/group, $N = 10$ rats/group). Significant difference between Wistar-SD vs. HTG-FRD rats, * $p < 0.05$, One-way ANOVA, Dunnett multiple comparisons test. For abbreviations, see Fig. 1.

One-way ANOVA, Tukey-Kramer multiple comparisons test; $n = 10$ rats/group; Wistar-SD $n = 23$ hippocampal slices, HTG-SD $n = 22$ hippocampal slices, HTG-FRD $n = 21$ hippocampal slices).

Synaptic plasticity was investigated by LTP induction at the CA3-CA1 synapse in the *stratum radiatum* of the hippocampus. Typical dendritic EPSP traces recorded before

HFS (100 Hz, 1 s), immediately after HFS, and 45 min after HFS are shown in Fig. 5A. HFS resulted into induction of LTP in the hippocampus of all three experimental groups. LTP maintenance (41–45 min after HFS) was significantly reduced in rats with FRD (Fig. 5B; $p < 0.05$ Wistar-SD vs. HTG-FRD, One way ANOVA, Dunnett comparison test; $n = 10$ rats/group; $n = 10$ hippocampal slices/group).

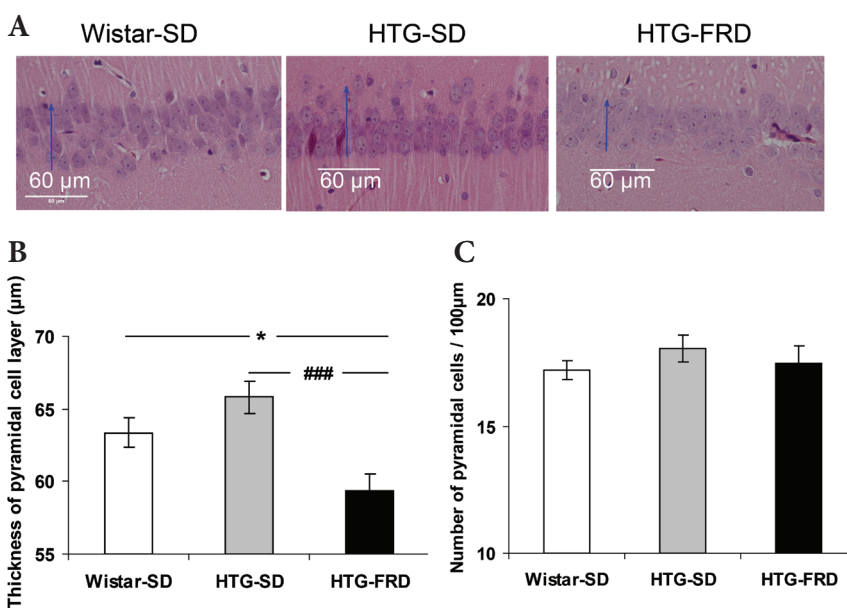


Figure 6. Effect of FRD on the thickness and number of pyramidal cells at the CA1 area of the rat hippocampus. **A.** Illustrative figures of hematoxylin-eosin stained hippocampal sections with focus on the pyramidal cell layer at the CA1 area of each experimental group. Insert: 60 μm . Arrows indicate the thickness of CA1 pyramidal cell layer. **B.** Graph shows the thickness of the pyramidal cell layer in micrometers. **C.** Graph shows the pyramidal cell density per 100 μm of the CA1 area length. Values are means \pm SEM of $n = 72$ in Wistar-SD, $n = 81$ in HTG-SD and $n = 72$ in HTG-FRD. Significant difference Wistar-SD vs. HTG-FRD, * $p < 0.05$; HTG-SD vs. HTG-FRD, ### $p < 0.001$, One-Way ANOVA, Tukey-Kramer multiple comparisons test. n , hippocampal sections. For more abbreviations, see Fig. 1.

Effect of FRD on the thickness and number of pyramidal cell layer in the CA1 area of the hippocampus

The number of pyramidal cells in the CA1 area of the hippocampus was calculated and the thickness of the pyramidal cell layer in this area was investigated ($n = 10$ rats/group; Wistar-SD $n = 72$ hippocampal sections; HTG-SD $n = 81$ hippocampal sections; HTG-FRD $n = 72$ hippocampal sections). Representative H-E stained samples of the pyramidal cell layer of the CA1 area in the rat hippocampus are shown in Fig. 6A. We found significantly reduced thickness of the pyramidal cell layer at the CA1 area of the hippocampus of HTG-FRD rats compared to both groups fed SD (Fig. 6B) ($p < 0.001$ HTG-SD vs. HTG-FRD; $p < 0.05$ Wistar-SD

vs. HTG-FRD; One way ANOVA, Tukey-Kramer multiple comparisons test; $p < 0.01$ Wistar-SD vs. HTG-SD and HTG-FRD, One-way ANOVA, Dunnett multiple comparisons test). The density of pyramidal cells in the CA1 area expressed as the number of cells *per* 100 μm did not differ among groups (Fig. 6C).

Correlations of neurological deficits with physiological status of rat

To support association of neurological dysfunction with FRD induced changes, correlations between the parameters measured were investigated (Fig. 7A–H). We found several middle correlations where ($0.3 < |r(x,y)| \leq 0.8$): LTP value

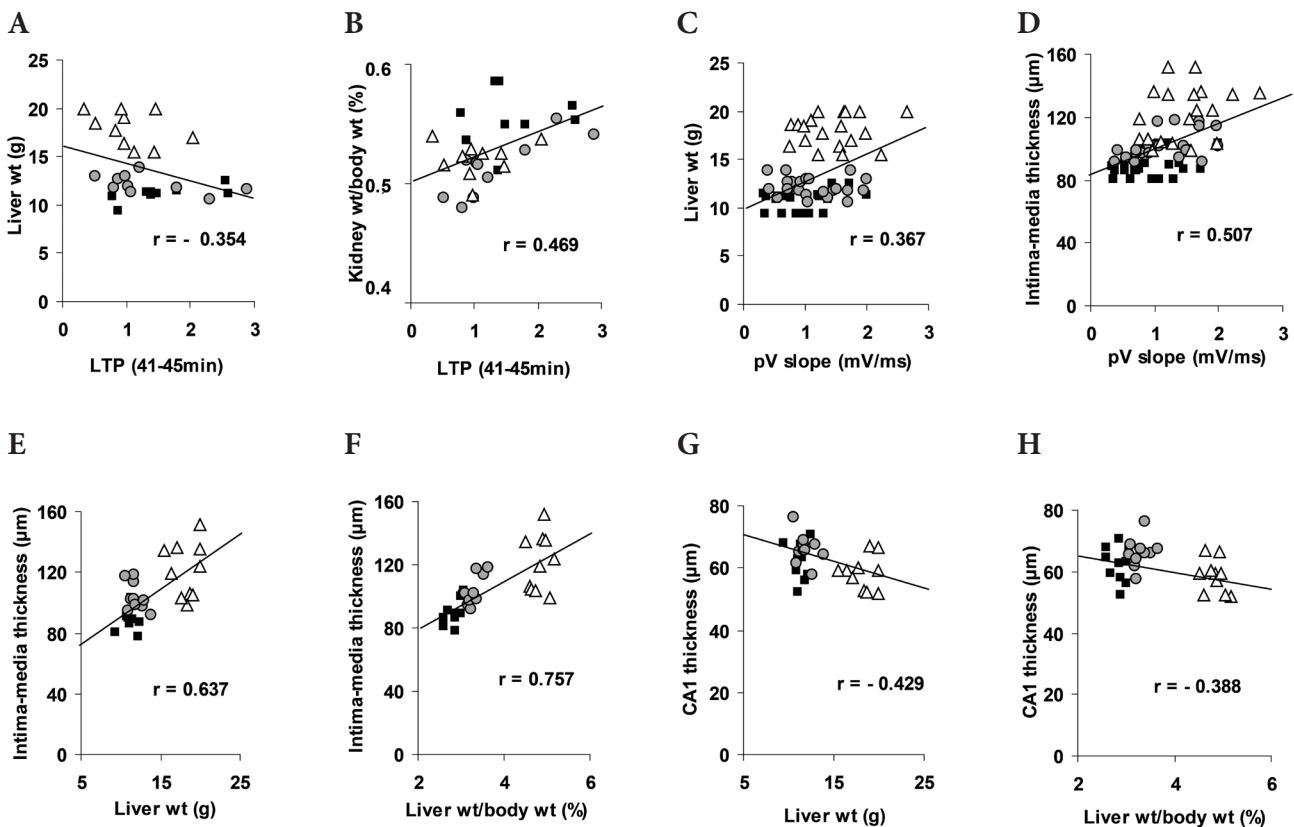


Figure 7. Correlations of individual electrophysiological, morphometrical and rat organ parameters with regard to metabolic syndrome. **A.** LTP at the rat hippocampus ($n = 10$ /group) inversely associated with liver weight. **B.** LTP at the rat hippocampus ($n = 10$ /group) directly associated with kidney wt/body wt ratio. **C.** pV slope at the rat hippocampus ($n = 22$ in Wistar-SD, $n = 23$ in HTG-SD and $n = 19$ in HTG-FRD) directly associated with liver weight. **D.** pV slope at rat hippocampus ($n = 22$ hippocampal slices in Wistar-SD, $n = 23$ in HTG-SD and $n = 19$ in HTG-FRD) directly associated with *intima-media* thickness of abdominal aorta. **E.** Liver weight directly associated with *intima-media* thickness of abdominal aorta ($n = 10$ rats/group). **F.** Liver wt/body wt ratio directly associated with *intima-media* thickness of abdominal aorta ($n = 10$ rats/group). **G.** Liver weight inversely associated with the thickness of pyramidal cell layer of CA1 area ($n = 10$ rats/group). **H.** Liver wt/body wt ratio inversely associated with the thickness of pyramidal cell layer of CA1 area ($n = 10$ rats/group). Correlations were determined by the correlation coefficient (r), where $0.3 < |r(x,y)| \leq 0.8$ was considered as middle correlation and $|r(x,y)| > 0.8$ was considered as high correlation (not found). Low correlation ($r < 0.3$) was found between PoS amplitude and parameters related to metabolic syndrome (not shown). ■ Wistar-SD; ● HTG-SD; △ HTG-FRD; n , hippocampal slices; wt, weight; pV, presynaptic fiber volley; LTP, long-term potentiation. For more abbreviations, see Fig. 1.

inversely correlated with liver weight ($r = -0.354$) (Fig. 7A) and directly correlated with kidney wt/body wt ratio ($r = 0.469$) (Fig. 7B); pV slope directly correlated with liver weight ($r = 0.367$) (Fig. 7C) and with *intima-media* thickness ($r = 0.507$) (Fig. 7D). Further, FRD-induced changes were associated with direct correlation of *intima-media* thickness with liver weight ($r = 0.637$) (Fig. 7E) and with liver wt/body wt ratio ($r = 0.757$) (Fig. 7F). Pyramidal cell layer thickness at the CA1 area inversely correlated with liver weight ($r = -0.429$) (Fig. 7G) and with liver wt/body wt ratio ($r = -0.388$) (Fig. 7H).

Discussion

Recently, it has been generally accepted that MetS is associated with central obesity, dyslipidemia, insulin resistance, hypertension, impaired glucose tolerance, increased risk of nonalcoholic fatty liver disease, kidney dysfunction, etc. (Simmons et al. 2010). In the present work, we observed that livers of HTG-FRD rats were highly overweight with signs of steatosis and increased liver wt/body wt ratio compared to rats fed SD. Accordingly, liver overweight and structural alterations of the liver were reported by Altunkaynak and Ozbek (2009) in female Sprague Dawley rats on FRD. The diet in their work was constituted highly of fat (30%) for 3 months and induced obesity. In our experiment, the weight gain did not significantly differ in HTG rats fed eight weeks a diet with added 1% cholesterol and 7.5% of lard compared to rats fed SD. Thus obesity was not induced but liver overweight was present. Obesity is one of the main factors in MetS. However, there are individuals with normal body mass index displaying with metabolic disorders, so called metabolically unhealthy non-obese ones. The non-alcoholic fatty liver disease, a common cause of chronic liver disease in the obese population, has been increasingly reported in the non-obese population (Yousef et al. 2017). Based on our present results, we suggest that HTG rats fed FRD could serve as an experimental tool in studying metabolically unhealthy non-obese individuals. Moreover, metabolically healthy obese individuals have a better cardiovascular prognosis compared with metabolically unhealthy non-obese patients who display except the nonalcoholic fatty liver disease other target organ damage, e.g. renal dysfunction and increased arterial stiffness (Lee et al. 2018).

MetS is leading to chronic kidney disease but its role in the progression has not been established (Prasad 2014). Even mild chronic kidney disease is associated with increased risk of cardiovascular diseases (Mann 2005). Here we show significantly lower kidney weight in both groups of HTG rats, without reference to diet. In the literature it was reported that high triacylglycerols may be nephrotoxic by promoting pro-inflammatory cytokine production (Wahba and Mak 2007).

A relationship between vessel *intima-media* thickness and MetS was reported in several works (Aydin et al. 2013; Reinehr et al. 2013; Rumińska et al. 2017). Similarly in the present work, we found significantly increased *intima-media* thickness associated with fat-rich diet. Wu and co-workers (2014) showed that carotid artery *intima-media* thickness increased significantly with steatohepatitis, which developed after 12 and 16 weeks of FRD in Sprague-Dawley rats. In their study correlations between the carotid *intima-media* thickness with hepatic inflammation score and steatosis score were shown in non-alcoholic fatty liver disease. Similarly, we found a correlation of rat liver weight with *intima-media* thickness and correlation of liver wt/body wt ratio with *intima-media* thickness in the present work. Ideal cardiovascular health was inversely associated with aortic *intima-media* thickness and directly associated with elasticity in adolescents (Pahkala et al. 2013). The influence of lifestyle modification, based primarily on lipid-lowering therapy with low-fat and low-cholesterol diet on atherosclerotic progression was confirmed by ultrasonographic change in the common carotid *intima-media* thickness (Markus et al. 1997). The major role is probably played by the enhanced systolic blood pressure in the changed *intima-media* thickness.

Neurological dysfunction as one of the potential signs of so-called metabolic cognitive syndrome has not been sufficiently explored yet. In our work we found that basal neurotransmission, characterized by somatic PoS and dendritic EPSP responses, did not differ in HTG rats compared to Wistar rats, irrespective of the diet. However, we observed FRD-induced impairment of synaptic plasticity, when increased EPSP slope due to HFS dropped to baseline values within about 15–20 min in HTG-FRD rats. In accordance with our results, reduced LTP was observed at the CA1 area of the hippocampus of obese Zucker rats (Alzoubi et al. 2005). There is evidence that rats maintained on diet-induced insulin resistance, i.e. high-fat high-glucose diet supplemented with high-fructose corn syrup, exhibited impaired spatial learning ability, reduced hippocampal dendritic spine density, and reduced LTP at the Schäffer collateral-CA1 synapse (Stranahan et al. 2008). A substantial decrease in LTP at the CA1 region of the hippocampus of C57BL/6J mice was proved by Liu and co-workers (2015) after 12-week fat-rich diet. On the same strain of mice with 12 weeks of FRD intake, a significant reduction in LTP magnitude was reported in the ventral hippocampus (Krishna et al. 2015). Farr and co-workers (2008) showed impaired maintenance of the N-methyl-D-aspartate component of the mouse hippocampal LTP due to triacylglycerols. Moreover, they found that triacylglycerols had a negative effect on cognition in obese mice, and impaired cognition was improved by targeting the decrease of triacylglycerols. An impairment of tetanus-induced LTP in CA1 of *ex-vivo* hippocampal

slices was reported by Koudinov and Koudinova (2001) on cholesterol (2%) fed rats vs. control animals.

Besides the LTP impairment in HTG-FRD rats, the second major finding arising from the electrophysiological part of this study is that FRD affects an afferent hippocampal function. The pV potential, an index of the density of afferent fibers recruited by the stimulation, was significantly increased as shown in the stimulus-response curve. This was found to be over the stimulation range in the stimulus-response curve of HTG-FRD rats compared to HTG-SD, suggesting increased presynaptic excitability due to FRD. Similar results concerning an increase of nerve fiber excitability were reported in streptozotocin-treated diabetic rats by Candy and Szatkowski (2000) who described a marked leftward shift in the pV slope shown in perforant pathway, mossy fibers, Schäffer collaterals and alveus of the stimulus-response curves compared to controls. In the traumatic brain injury model, reduced CA3 fiber excitability and reduced CA1 synaptic strength at ipsilateral hippocampus observed within 48 h after cortical contusion injury seems to be obvious (Norris and Scheff 2009), but on the other side, alteration of the pV, as a measure of viability of presynaptic fibers, was not changed by age (Jouvenneau et al. 1998; Potier et al. 2000) or by global rat brain ischemia on day 3 after surgery (Takeuchi et al. 2015). In accordance with experiments performed on diabetic rats (Candy and Szatkowski 2000), in the present work we found no difference in stimulus-response curves of basal neurotransmission parameters, thus either in the PoS amplitude or in the EPSP slope in HTG-FRD rats compared to rats fed SD. An increased presynaptic excitability (pV slope) did not result in expected and corresponding increase in postsynaptic excitability (EPSP slope). Moreover, not only FRD but also high-fructose feeding for 7 weeks resulted in impaired synaptic plasticity and increased pV amplitude in the mouse hippocampus (Cisternas et al. 2015). Similarly as did Candy and Szatkowski (2000) suggest in the diabetes study, we also incline to the opinion that some inhibitory neuromodulators may be involved in this paradoxical phenomenon. Recently, attention has been given to neuron-astrocyte communication as the astrocytes could be fundamental players in the regulation of synaptic transmission and plasticity (Guerra-Gomes et al. 2018).

Functional changes due to FRD in the hippocampus directed us to study possible morphological changes in this brain structure. In the present work we showed reduced thickness of the pyramidal cell layer at the CA1 area. As the reduction of the pyramidal cell layer thickness was not accompanied with reduction of the pyramidal cell number, it may suggest that the size of pyramidal cells was slightly diminished. Shrinkage of pyramidal cells was reported as a result of high cholesterol diet in the hippocampal CA1 area of adult and aged rats also in the recent study of Abo El-Khair and co-workers (2014). Calvo-Ochoa and co-

authors (2014) showed that even short-term (7-day-lasting) high-fat-and-fructose diet induced decreased weight of the hippocampus, reduction in dendritic arborization and decreased dendritic spine number in the CA1 area, as well as changes in hippocampal astrocytes and microglia. Alarming data were presented also by Yau and co-workers (2012) who studied the impact of MetS on the brain of human obese adolescents where those with MetS showed not only smaller hippocampal volumes but also lower arithmetic, spelling, attention, and mental flexibility and a trend for lower overall intelligence.

Finally, several correlations between neuronal dysfunctions and physiological or morphological alterations elicited by FRD were found (Fig. 7). The strongest observed correlation of neurological dysfunction and physiological status was a direct association of pV slope with aortic *intima-media* thickness ($r = 0.507$). The best correlations between the MetS risk factors tested were direct correlation of *intima-media* thickness with liver weight ($r = 0.637$) and *intima-media* thickness with liver wt/body wt ratio ($r = 0.757$).

In conclusion, even though obesity was not present in HTG-FRD rats, marked morphological alterations in the liver, such as hepatomegaly with the presence of steatosis, were observed as a result of FRD. Based on this observation as well as on results presented in our previous work (Kaprinay et al 2016), HTG rats on FRD could serve as an experimental tool for the study of metabolically unhealthy non-obese individuals. The fat-rich diet-induced thickening of the abdominal aorta wall suggests most likely impaired vascular elasticity. Moreover, our results indicate that the FRD interferes with brain function. Aggravated synaptic plasticity was found in the hippocampus of rats on FRD and on the contrary, increased presynaptic activity was observed. Hippocampal functional changes were accompanied with reduced thickness of the pyramidal cell layer at the CA1 area of the hippocampus. LTP was inversely associated with liver weight. The slope of pV was directly associated with liver weight and aortic *intima-media* thickness. These results suggest association of the impaired vessel wall and the overweight liver with neurological deficits, thus possible conditions leading to the consecutive development of metabolic cognitive syndrome. The presented findings are not only of experimental significance but due to the increased incidence of metabolic diseases worldwide, they could be beneficial in terms of spreading education about negative effects of a FRD and thus promoting a healthy diet and healthy lifestyle.

Acknowledgement. This work was supported by the Ministry of Education, Science, Research and Sport of the Slovak Republic (grant number VEGA 2/0054/15). The authors thank Mrs. Katarina Vandakova, Mrs. Monika Srnova and Mrs. Julia Polakova for their technical assistance.

Conflict of Interest. The authors declare that there are no conflicts of interest.

References

- Abo El-Khair DM, El-Safti Fel-N, Nooh HZ, El-Mehi AE (2014): A comparative study on the effect of high cholesterol diet on the hippocampal CA1 area of adult and aged rats. *Anat. Cell. Biol.* **47**, 117–126
<https://doi.org/10.5115/acb.2014.47.2.117>
- Abramoff MD, Magalhaes PJ, Ram SJ (2004): Image processing with ImageJ. *Biophotonics Internat.* **11**, 36–42
- Altunkaynak BZ, Ozbek E (2009): Overweight and structural alterations of the liver in female rats fed a high-fat diet: a stereological and histological study. *Turk. J. Gastroenterol.* **20**, 93–103
- Alzoubi KH, Aleisa AM, Alkadhi KA (2005): Impairment of long-term potentiation in the CA1, but not dentate gyrus, of the hippocampus in obese Zucker rats: role of calcineurin and phosphorylated CaMKII. *J. Mol. Neurosci.* **27**, 337–346
<https://doi.org/10.1385/JMN:27:3:337>
- Aydin M, Bulur S, Alemdar R, Yalçın S, Türker Y, Basar C, Aslantas Y, Yazgan O, Albayrak S, Özhan H (2013): The impact of metabolic syndrome on carotid intima media thickness. *Eur. Rev. Med. Pharmacol. Sci.* **17**, 2295–2301
- Boitard C, Etchamendy N, Sauvans J, Aubert A, Tronel S, Marighetto A, Layé S, Ferreira G (2012): Juvenile, but not adult exposure to high-fat diet impairs relational memory and hippocampal neurogenesis in mice. *Hippocampus* **22**, 2095–2100
<https://doi.org/10.1002/hipo.22032>
- Calvo-Ochoa E, Hernandez-Ortega K, Ferrera P, Morimoto S, Arias C (2014): Short-term high-fat-and-fructose feeding produces insulin signaling alterations accompanied by neurite and synaptic reduction and astroglial activation in the rat hippocampus. *J. Cereb. Blood Flow Metab.* **34**, 1001–1008
<https://doi.org/10.1038/jcbfm.2014.48>
- Candy SM, Szatkowski MS (2000): Neuronal excitability and conduction velocity changes in hippocampal slices from streptozotocin-treated diabetic rats. *Brain Res.* **863**, 298–301
[https://doi.org/10.1016/S0006-8993\(00\)02171-5](https://doi.org/10.1016/S0006-8993(00)02171-5)
- Cisternas P, Salazar P, Serrano FG, Montecinos-Oliva C, Arredondo SB, Varela-Nallar L, Barja S, Vio CP, Gomez-Pinilla F, Inestrosa NC (2015): Fructose consumption reduces hippocampal synaptic plasticity underlying cognitive performance. *Biochim. Biophys. Acta* **1852**, 2379–2390
<https://doi.org/10.1016/j.bbadis.2015.08.016>
- Craft S (2005): Insulin resistance syndrome and Alzheimer's disease: age- and obesity-related effects on memory, amyloid, and inflammation. *Neurobiol. Aging* **26**, S65–69
<https://doi.org/10.1016/j.neurobiolaging.2005.08.021>
- Fanjiang G, Kleinman RE (2007): Nutrition and performance in children. *Curr. Opin. Clin. Nutr. Metab. Care* **10**, 342–347
<https://doi.org/10.1097/MCO.0b013e3280523a9e>
- Farr SA, Yamada KA, Butterfield DA, Abdul HM, Xu L, Miller NE, Banks WA, Morley JE (2008): Obesity and hypertriglyceridemia produce cognitive impairment. *Endocrinology* **149**, 2628–2636
<https://doi.org/10.1210/en.2007-1722>
- Gasparova Z, Stara V, Stolc S (2014): Effect of antioxidants on functional recovery after in vitro-induced ischemia and long-term potentiation recorded in the pyramidal layer of the CA1 area of rat hippocampus. *Gen. Phys. Biophys.* **33**, 43–52
https://doi.org/10.4149/gpb_2013062
- Grundy SM (2007): Metabolic syndrome: a multiplex cardiovascular risk factor. *J. Clin. Endocrinol. Metab.* **92**, 399–404
<https://doi.org/10.1210/jc.2006-0513>
- Grundy SM, Cleeman JI, Daniels SR, Donato KA, Eckel RH, Franklin BA, Gordon DJ, Krauss RM, Savage PJ, et al. (2005): Diagnosis and management of the metabolic syndrome: an American Heart Association/National Heart, Lung and Blood Institute scientific statement. *Circulation* **112**, 2735–2752
<https://doi.org/10.1161/CIRCULATIONAHA.105.169404>
- Guerra-Gomes S, Sousa N, Pinto L, Oliveira JF (2018): Functional roles of astrocyte calcium elevations: from synapses to behavior. *Front. Cell. Neurosci.* **11**, 427
<https://doi.org/10.3389/fncel.2017.00427>
- Hansen BC, Landsberg L, Bray GA (2008): The sympatho-adrenal system in the metabolic syndrome. In: *The Metabolic Syndrome: Epidemiology, Clinical Treatment, and Underlying Mechanisms*. (Eds. BC Hansen and GA Bray), pp. 85–104, Humana Press, Totowa, NJ
<https://doi.org/10.1007/978-1-60327-116-5>
- Hassenstab JJ, Sweat V, Bruehl H, Convit A (2010): Metabolic syndrome is associated with learning and recall impairment in middle age. *Dement. Geriatr. Cogn. Disord.* **29**, 356–362
<https://doi.org/10.1159/000296071>
- Huang PL (2005): Unraveling the links between diabetes, obesity, and cardiovascular disease. *Circ. Res.* **96**, 1129–1131
[https://doi.org/10.1002/\(SICI\)1098-1063\(1998\)8:6<627::AID-HIPO5>3.0.CO;2-X](https://doi.org/10.1002/(SICI)1098-1063(1998)8:6<627::AID-HIPO5>3.0.CO;2-X)
- Huang PL (2009): A comprehensive definition for metabolic syndrome. *Dis. Model Mech.* **2**, 231–237
<https://doi.org/10.1242/dmm.001180>
- Hwang LL, Wang CH, Li TL, Chang SD, Lin LC, Chen CP, Chen CT, Liang KC, Ho IK, Yang WS, Chiou LC (2010): Sex differences in high-fat diet-induced obesity, metabolic alterations and learning, and synaptic plasticity deficits in mice. *Obesity* **18**, 463–469
<https://doi.org/10.1038/oby.2009.273>
- Jouveneau A, Dutar P, Billard JM (1998): Alteration of NMDA receptor-mediated synaptic responses in CA1 area of the aged rat hippocampus: contribution of GABAergic and cholinergic deficits. *Hippocampus* **8**, 627–637
[https://doi.org/10.1002/\(SICI\)1098-1063\(1998\)8:6<627::AID-HIPO5>3.0.CO;2-X](https://doi.org/10.1002/(SICI)1098-1063(1998)8:6<627::AID-HIPO5>3.0.CO;2-X)
- Kahn R, Buse J, Ferrannini E, Stern M (2005): The metabolic syndrome: time for a critical appraisal. Joint statement from the American Diabetes Association and the European Association for the Study of Diabetes. *Diabetologia* **48**, 1684–1699
<https://doi.org/10.1007/s00125-005-1876-2>
- Kanoski SE, Davidson TL (2010): Different patterns of memory impairments accompany short- and longer-term maintenance on a high-energy diet. *J. Exp. Psychol. Anim. Behav. Process.* **36**, 313–319
<https://doi.org/10.1037/a0017228>
- Kaprinay B, Liptak B, Slovak L, Svik K, Knezl V, Sotnikova R, Gasparova Z (2016): Hypertriglyceridemic rats fed high fat diet as a model of metabolic syndrome. *Physiol. Res.* **65**, S515–S518

- Koudinov AR, Koudinova NV (2001): Essential role of cholesterol in synaptic plasticity and neuronal degeneration. *FASEB J.* **15**, 1858–1860
<https://doi.org/10.1096/fj.00-0815fje>
- Krishna S, Keralapurath MM, Lin Z, Wagner JJ, de La Serre CB, Harn DA, Filipov NM (2015): Neurochemical and electrophysiological deficits in the ventral hippocampus and selective behavioral alterations caused by high-fat diet in female C57BL/6 mice. *Neuroscience* **297**, 170–181
<https://doi.org/10.1016/j.neuroscience.2015.03.068>
- Lee HJ, Kim HL, Chung J, Lim WH, Seo JB, Kim SH, Zo JH, Kim MA (2018): Interaction of metabolic health and obesity on subclinical target organ damage. *Metab. Syndr. Rel. Dis.* **16**, 1–8
<https://doi.org/10.1089/met.2017.0078>
- Lehnen AM, Rodrigues B, Irigoyen MC, De Angelis K, D'Agord Schaan B (2013): Cardiovascular changes in animal models of metabolic syndrome. *J. Diabetes Res.* **2013**, 761314
<https://doi.org/10.1155/2013/761314>
- Liquori GE, Calamita G, Cascella D, Mastrodonato M, Portincasa P, Ferri D (2009): An innovative methodology for the automated morphometric and quantitative estimation of liver steatosis. *Histol. Histopathol.* **24**, 49–60
- Liu Z, Patil IY, Jiang T, Sancheti H, Walsh JP, Stiles BL, Yin F, Cadenas E (2015): High-fat diet induces hepatic insulin resistance and impairment of synaptic plasticity. *PLoS One* **10**, e0128274
<https://doi.org/10.1371/journal.pone.0128274>
- Mann JF (2005): Cardiovascular risk in patients with mild renal insufficiency: implications for the use of ACE inhibitors. *Presse Med.* **34**, 1303–1308
[https://doi.org/10.1016/S0755-4982\(05\)84178-8](https://doi.org/10.1016/S0755-4982(05)84178-8)
- Markus RA, Mack WJ, Azen SP, Hodis HN (1997): Influence of lifestyle modification on atherosclerotic progression determined by ultrasonographic change in the common carotid intima-media thickness. *Am. J. Clin. Nutr.* **65**, 1000–1004
<https://doi.org/10.1093/ajcn/65.4.1000>
- Muller M, Tang MX, Schupf N, Manly JJ, Mayeux R, Luchsinger JA (2007): Metabolic syndrome and dementia risk in a multiethnic elderly cohort. *Dement. Geriatr. Cogn. Disord.* **24**, 185–192
<https://doi.org/10.1159/000105927>
- Noble EE, Hsu TM, Kanoski SE (2017): Gut to Brain Dysbiosis: Mechanisms linking western diet consumption, the microbiome, and cognitive impairment. *Front. Behav. Neurosci.* **11**, 9
<https://doi.org/10.3389/fnbeh.2017.00009>
- Norris CM, Scheff SW (2009): Recovery of afferent function and synaptic strength in hippocampal CA1 following traumatic brain injury. *J. Neurotrauma* **26**, 2269–2278
<https://doi.org/10.1089/neu.2009.1029>
- Pahkala K, Hietalampi H, Laitinen TT, Viikari JS, Rönnemaa T, Niinikoski H, Lagström H, Talvia S, Jula A, Heinonen OJ, et al. (2013): Ideal cardiovascular health in adolescence: effect of lifestyle intervention and association with vascular intima-media thickness and elasticity. *Circulation* **127**, 2088–2096
<https://doi.org/10.1161/CIRCULATIONAHA.112.000761>
- Panza F, Solfrizzi V, Logroscino G, Maggi S, Santamato A, Seripa D, Pilotto A (2012): Current epidemiological approaches to the metabolic-cognitive syndrome. *J. Alzheimers Dis.* **30**, S31–75
<https://doi.org/10.3233/JAD-2012-111496>
- Paschos P, Paletas K (2009): Non alcoholic fatty liver disease and metabolic syndrome. *Hippokratia* **13**, 9–19
- Potier B, Poindessous-Jazat F, Dutar P, Billard JM (2000): NMDA receptor activation in the aged rat hippocampus. *Experimental. Gerontol.* **35**, 1185–1199
[https://doi.org/10.1016/S0531-5565\(00\)00122-4](https://doi.org/10.1016/S0531-5565(00)00122-4)
- Prasad GVR (2014): Metabolic syndrome and chronic kidney disease: Current status and future directions. *World J. Nephrol.* **3**, 210–219
<https://doi.org/10.5527/wjn.v3.i4.210>
- Reaven GM (1988): Banting lecture 1988. Role of insulin resistance in human disease. *Diabetes* **37**, 1595–1607
<https://doi.org/10.2337/diab.37.12.1595>
- Reinehr T, Wunsch R, Putter C, Scherag A (2013): Relationship between carotid intima-media thickness and metabolic syndrome in adolescents. *J. Pediatr.* **163**, 327–332
<https://doi.org/10.1016/j.jpeds.2013.01.032>
- Rumińska M, Witkowska-Sędek E, Majcher A, Brzewski M, Czerwonogrodzka-Senczyzna A, Demkow U, Pyrzak B (2017): Carotid intima-media thickness and metabolic syndrome components in obese children and adolescents. *Adv. Exp. Med. Biol.* **1021**, 63–72
<https://doi.org/10.1007/s00125-009-1620-4>
- Schwarz NF, Nordstrom LK, Pagen LHG, Palombo DJ, Salat DH, Milberg WP, McGlinchey RE, Leritz EC (2017): Differential associations of metabolic risk factors on cortical thickness in metabolic syndrome. *Neuroimage Clin.* **17**, 98–108
<https://doi.org/10.1016/j.nicl.2017.09.022>
- Siervo M, Harrison SL, Jagger C, Robinson L, Stephan BC (2014): Metabolic syndrome and longitudinal changes in cognitive function: a systematic review and meta-analysis. *J. Alzheimers Dis.* **41**, 151–161
<https://doi.org/10.3233/JAD-132279>
- Simmons RK, Alberti KGMM, Gale EAM, Colagiuri S, Tuomilehto J, Qiao Q, Ramachandran A, Tajima N, Brajkovich Mirchov I, Ben-Nakhi A, et al. (2010): The metabolic syndrome: useful concept or clinical tool? Report of a WHO expert consultation. *Diabetologia* **53**, 600–605
<https://doi.org/10.1007/s00125-009-1620-4>
- Sjögren M, Blennow K (2005): The link between cholesterol and Alzheimer's disease. *World J. Biol. Psychiatry* **6**, 85–97
<https://doi.org/10.1080/15622970510029795>
- Stranahan AM, Norman ED, Lee K, Cutler RG, Telljohann RS, Egan JM, Mattson MP (2008): Diet-induced insulin resistance impairs hippocampal synaptic plasticity and cognition in middle-aged rats. *Hippocampus* **18**, 1085–1088
<https://doi.org/10.1002/hipo.20470>
- Takeuchi K, Yang Y, Takayasu Y, Gertner M, Hwang JY, Aromolaran K, Bennett MV, Zukin RS (2015): Estradiol pretreatment ameliorates impaired synaptic plasticity at synapses of insulted CA1 neurons after transient global ischemia. *Brain Res.* **1621**, 222–230
<https://doi.org/10.1016/j.brainres.2014.11.016>
- Tonar Z, Kochova P, CimrmanR, Perktold J, Witter K (2015): Segmental differences in the orientation of smooth muscle cells in the tunica media of porcine aortae. *Biomech. Model. Mechanobiol.* **14**, 315–332
<https://doi.org/10.1007/s10237-014-0605-5>

- Valladolid-Acebes I, Merino B, Principato A, Fole A, Barbas C, Lorenzo MP, García A, Del Olmo N, Ruiz-Gayo M, Cano V (2012): High-fat diets induce changes in hippocampal glutamate metabolism and neurotransmission. *Am. J. Physiol. Endocrinol. Metab.* **302**, E396–402
<https://doi.org/10.1152/ajpendo.00343.2011>
- Vance JE (2012): Dysregulation of cholesterol balance in the brain: contribution to neurodegenerative diseases. *Dis. Model. Mech.* **5**, 746–755
<https://doi.org/10.1242/dmm.010124>
- Wahba IM, Mak RH (2007): Obesity and obesity-initiated metabolic syndrome: mechanistic links to chronic kidney disease. *Clin. J. Am. Soc. Nephrol.* **2**, 550–562
<https://doi.org/10.2215/CJN.04071206>
- Wu J, Zhang H, Zheng H, Jiang Y (2014): Hepatic inflammation scores correlate with common carotid intima-media thickness in rats with NAFLD induced by a high-fat diet. *BMC Vet. Res.* **10**, 162–171
<https://doi.org/10.1186/1746-6148-10-162>
- Yau PL, Castro MG, Tagani A, Tsui WH, Convit A (2012): Obesity and metabolic syndrome and functional and structural brain impairments in adolescence. *Pediatrics* **130**, e856–864
<https://doi.org/10.1542/peds.2012-0324>
- Yousef MH, Al Juboori A, Albarrak AA, Ibdah JA, Tahan V (2017): Fatty liver without a large „belly“: Magnified review of non-alcoholic fatty liver disease in non-obese patients. *World J. Gastrointest. Pathophysiol.* **8**, 100–107
<https://doi.org/10.4291/wjgp.v8.i3.100>
- Zicha J, Pechanova O, Cacanyova S, Cebova M, Kristek F, Török J, Simko F, Dobesova Z, Kunes J (2006): Hereditary hypertriglyceridemic rat: a suitable model of cardiovascular disease and metabolic syndrome? *Physiol. Res.* **55**, 49–63

Received: October 20, 2017

Final version accepted: May 21, 2018

First published online: October 17, 2018